Preprints of the 19th World Congress
The International Federation of Automatic Control
Cape Town, South Africa. August 24-29, 2014

Real-Time 3D Collision Prediction for On-Orbit Servicing Missions

A. Posch*, M. Schmidt*, A. O. Schwientek, J. Sommer**, W. Fichter***

**Institute of Flight Mechanics and Control, Universitaet Stuttgart, Stuttgart, Germany (e-mail: andre.posch@ifr.uni-stuttgart.de).*
***ASTRIUM GmbH, Bremen, Germany (e-mail: josef.sommer@astrium.eads.net).*

Abstract: Due to an increasing amount of large space debris and the attractive perspective of repairing or refilling valuable satellites on orbit, rendezvous missions are a growing field of interest. The worst case for a rendezvous is the collision of both satellites and therefore precautions have to be taken to avoid unwanted contact even in case of system outage. A new approach to real-time collision prediction incorporating navigation uncertainties and disturbances like airdrag and J2 gravity in full 3d is presented which is even tuned for feasibility of on-board implementation.

Keywords: Satellite Rendezvous, Collision Probability, Safety, Collision Prediction

1. INTRODUCTION

With the growing number of uncontrollable satellites in Earth orbit the demand for in orbit satellite repair, refill, inspection or broken satellite disposal is increasing dramatically in recent times. For those servicing tasks rendezvous mission concepts with high degress of autonomy are under investigation by agencies around the world, e.g. DARPA's Phoenix (see Barnhart (2012)), DLR's DEOS (see Reintsema et al. (2010)) or USAF's ARAPAIMA (see Harris et al. (2011)).

The worst case for a rendezvous mission is a collision between the servicer satellite and the client satellite. This can e.g. happen if the servicer satellite has a malfunction and does not respond to commands for some time. One common approach is to use an e/i separation scheme described in Montenbruck et al (2004) for the approach trajectory which prevents the servicer from drifting into the client if control is lost.

Many papers elaborate collision predictors for fly-by maneuvers, e.g. Akella and Alfriend (2000), but safety studies for rendezvous missions are rare. A discussion of this problem can be found in Slater et al (2006).

To verify if the current motion state is safe for a certain number of orbits even under impact of navigation errors, a new method using a prediction of the navigation filter state and covariance for several orbits under free flight condition is developed. This new method uses full 3d information in contrary to most classical approaches to take into account the full shape and orientation of the uncertainty ellipsoid.

Two tests for collision are implemented, first a test for the distance between the ellipsoid defined by the covariance and the client satellite and a test of the 3d integral of the client volume in the multivariate gaussian distribution given by the covariance. An iterative trajectory propagation approach together with the two step collision distance / probability test ensures the applicabilty of algorithm to an onboard implemention with limited computational effort.

The organization of the paper is as follows: The rendezvous scenario and the investigated nominal trajectory is described in Section 2, followed by an overview of the proposed motion state safety monitoring concept in Section 3. The fundamental models and the collision prediction algorithms are described in detail in Section 4 and performance evaluation is given in Section 5. Finally the conclusion and future work is presented in Section 6.

2. SCENARIO

The focus for the application of the proposed algorithm is as follows, but this does not exclude application to different approach scenarios.

"Client" describes the satellite that has to be serviced and is usually passive without the possibility to communicate and receive commands, which means e.g. relative GPS is not available. "Servicer" is the satellite that is going to repair/refill/remove the client satellite.

In this scenario but without loss of generality both satellites are assumed to fly in a low earth orbit (LEO) at an altitude of about 400 km (where airdrag is one of the major trajectory disturbances) at a high inclination which makes the impact of J2 gravity a major disturbance as well. For the initial approach the separation between the two satellites is about 10 km alongtrack in a presumably safe e/i separated formation, with the servicer flying behind the client satellite.

After receiving the go command the servicer spirals towards the client, reducing the size of the e/i separation ellipse until it reaches a hold point in 1 km distance. This part of the trajectory (the far range approach) is the typical application for the proposed collision prediction method.

In case of a malfunction of the servicer thrusters or a shutdown of the servicer navigation / guidance / control it is important that the servicer is not drifting into the client satellite. The e/i separation should prevent this, but in several cases, e.g. in case of bad navigation performance (e.g. due to bad illumination condition when using optical navigation) the amount of separation might be less then expected.

Therefore it is important to test the current motion state together with the currently estimated navigation performance for collision safety.

3. MOTION STATE SAFETY MONITORING CONCEPT

3.1 State and State Estimation Error Covariance Prediction

Based on the current state, the relative free flying trajectory (assuming no maneuvers) for n orbits is calculated along with the estimated navigation error with a reasonable temporal resolution. The initial state x and initial estimated navigation error covariance is supplied by the navigation filter. The relative state is described by the relative orbital elements (ROE) of the two satellites. The state and the navigation error at any time can be evaluated using the solution to the ROE equations which allow inclusion of airdrag and J2 gravity.

To reduce the computational effort, an iterative approach to find the time of highest collision risk is employed. After a rough scanning of the trajectory, the section with the highest risk is tested with a higher temporal resolution.

3.2 Collision Tests

At each time step the covariance ellipsoid and standard deviation sigma is evaluated and the minimum distance between the ellipsoid surface and the client is calculated as an indicator for a high collision risk. If the client is inside the ellipsoid the true probability is calculated using the integral of the client in the 3d probability density function defined by the current covariance. If the probability is above some threshold a collision warning is reported and eventually a critical abort maneuver initiated.

4. MODELS AND ALGORITHMS

4.1 Prediction and Test Process

4.1.1 Orbital model

The relative state of both satellites is described using the ROE formulation (see D'Amico 2010 for a good introduction) where the relative motion of the servicer with respect to the client is represented by six relative orbital elements similar to the six absolute Keplerian elements for Keplerian motion.

The set of ROEs $\delta\mathbf{a}$ is given by $\delta\mathbf{a} = \begin{bmatrix} \delta a & \delta\lambda & \delta e_x & \delta e_y & \delta i_x & \delta i_y \end{bmatrix}$ using the dimension-less relative semi-major axis δa, the relative mean longitude between the spacecrafts $\delta\lambda$, the relative eccentricities δe_x, δe_y and the relative inclinations δi_x, δi_y (see D'Amico (2005)). The relative inclinations indicate the difference between the two absolute inclinations of the servicer's and the clients' orbits; the relative eccentricities indicate the difference between the two absolute eccentricities of the servicer's and the clients' orbits (see Montenbruck et al (2004)).

The current relative state $\mathbf{x}(t)$ in local vertical local horizontal (LVLH) frame (+X along track, +Y perpendicular to orbital plane, +Z downwards) at any time can easily be calculated from the ROEs at some initial time using the position of the client on the orbit $u = u(t) = \int \omega_0 \mathrm{d}t$ and $\mathrm{cu} = \cos(u), \mathrm{su} = \sin(u), \Delta u = u - u_0$:

$$\mathbf{x}_{\mathrm{LVLH}} = a \cdot \underbrace{\begin{bmatrix} \mathrm{cu} & 1 & 0 & 0 & -\mathrm{su} & 0 \\ -2\mathrm{su} & 3/2\cdot(\Delta u) & -1 & 0 & -2\mathrm{cu} & 0 \\ 0 & 0 & 0 & \mathrm{cu} & 0 & -\mathrm{su} \\ -\mathrm{su}\omega_0 & 0 & 0 & 0 & -\mathrm{cu}\omega_0 & 0 \\ -2\mathrm{cu}\omega_0 & -3/2\cdot\omega_0 & 0 & 0 & 2\mathrm{su}\omega_0 & 0 \\ 0 & 0 & 0 & -\mathrm{su}\omega_0 & 0 & -\mathrm{cu}\omega_0 \end{bmatrix}}_{\mathbf{T}_{\mathrm{ROE}\to\mathrm{LVLH}}} \delta\mathbf{a} \quad (1)$$

A big advantage over the formulation of the state in LVLH frame is the handy consideration of the J2 gravity perturbation which becomes very complicated otherwise (see Hayman (2012)). J2 is the impact of the earth's oblateness effect which leads to a change of the orbit depending on the inclination. The scenario investigated here has a high inclination of about 85 degrees. The influence of the perturbation is in this case not to be neglected. The J2 effect pertubs the ROEs and the effect on the ROEs $\delta\delta\mathbf{a}_{J_2}$ can be described by (see D'Amico (2010)):

$$\delta\delta\mathbf{a}_{J_2}(u) = \begin{bmatrix} \delta a \\ \delta\lambda - 21/2\cdot\gamma\sin(2i)\delta i_x\Delta u \\ \delta e\cos(\varphi + \varphi'\Delta u) \\ \delta e\sin(\varphi + \varphi'\Delta u) \\ \delta i_x \\ \delta i_y + 3\gamma\sin^2(i)\delta i_x\Delta u \end{bmatrix} \quad (2)$$

The new introduced variables are the gravitational effect $\gamma = J_2/2\cdot(R_E/a)^2$, with the earth oblateness factor $J_2 \approx 0{,}00108$, the earth's equatorial radius $R_E = 6378137\mathrm{m}$, the absolute inclination of the client i, the relative perigee $\varphi = \mathrm{atan2}(\delta e_y, \delta e_x)$, the deviation of the relative perigee $\varphi' = 3/2\cdot\gamma(5\cdot\cos^2(i) - 1)$, the relative eccentricity vector $\delta\mathbf{e} = \sqrt{\delta e_x^{\,2} + \delta e_y^{\,2}}$, the inclination of the orbit i and the semi-major axis a. The second major disturbance is the differential airdrag of the satellites. The impact of the differential airdrag on the ROEs can approximately be included by (see D'Amico (2010)):

$$\delta\delta\mathbf{a}_{\Delta d}(u) = 1/a\cdot\begin{bmatrix} -\dfrac{\Delta B\rho v^2\Delta u}{n^2} & \dfrac{3\cdot\Delta B\rho v^2\Delta u^2}{\left(4\cdot n^2\right)} & 0 & 0 & 0 & 0 \end{bmatrix}' \quad (3)$$

This results in $\delta\mathbf{a}_P(u) = \delta\mathbf{a}(u_0) + \delta\delta\mathbf{a}_{J_2}(u) + \delta\delta\mathbf{a}_{\Delta d}(u)$. It has to be noted that the airdrag is only known roughly because of uncertainties in air density and reference areas..

4.1.2 Propagation

The state at a certain time step is given by (1) and using the same transformation matrix the navigation error covariance at

a certain time step is given by (airdrag and J2 is only considered for the state propagation):

$$\mathbf{P}_{\mathrm{ROE}}(\mathbf{x}(t)) = \mathbf{T}_{\mathrm{LVLH}\to\mathrm{ROE}}\,\mathrm{cov}(\mathbf{x}(t_0))\mathbf{T}^{T}_{\mathrm{LVLH}\to\mathrm{ROE}} \quad (4)$$

The collision prediction period $t_{\mathrm{Sim}} = n_O \cdot t_O$. is given by the number of predicted orbits n_O times the duration of one orbit $t_O = 2\pi\omega_0$. To gain reliable information about the safety distance using numerical simulation, it is necessary to choose a very fine subdividision for the prediction time span. At each time step the collision risk has to be evaluated. The time between two consecutive steps is $t_{\mathrm{step}} = t_O / n_{sO}$ with the number of nominal steps per orbit n_{sO}. With a larger stepping the risk to miss a potential collision is increased. Using a sufficient small step size the risk to miss a possible collision is dramatically reduced but still there.

4.1.3 Iteration Process

Depending on the state it is possible to reduce the number of steps per orbit dramatically: The distance d from the client to the covariance ellipsoids surface over the time is used as an iteration indicator $\kappa = |d / K|$ with an appropriate scaling factor K (e.g. $K = 5$). The step time depending on κ is then calculated to $t_{\mathrm{step}}(\kappa) = t_{\mathrm{Sim}} \cdot \kappa / (n_{sO} \cdot n_O)$. κ is upper bounded to avoid missing a collision due to extremely large step sizes. But as mentioned above it is still possible to not find the global optimum for the shortest distance with this method. The iterative approach typically leads to a reduction of factor 20 while still having sufficient resolution at critical parts of the trajectory.

4.2 Covariance Ellipsoid Test

4.2.1 Covariance Ellipsoid

The following is under the assumption that the covariance matrix is symmetric and diagonalizable. Only the matrix elements which represent the relative position states are considered (but the impact of the velocity states is already included in the propagation).

With these ingredients, the covariance matrix is represented by an ellipsoid of the form $\boldsymbol{\rho}_1^{\,2} / \lambda_1^{\,2} + \boldsymbol{\rho}_2^{\,2} / \lambda_2^{\,2} + \boldsymbol{\rho}_3^{\,2} / \lambda_3^{\,2} - 1 = 0,$ where λ_i are the eigenvalues and $\boldsymbol{\rho}_i$ the normalized eigenvectors of equation, see Eberly (2011). The eigenvector $\boldsymbol{\rho}_i$ points into the direction of the semi-principal axes of the ellipsoid. The length of the semi-principal axes is given by $\sqrt{k\lambda_i}$, with a constant k.

The ellipsoid can now be interpreted as the servicer's position estimation error-ellipsoid, where the probability, that the servicer is inside of this ellipsoid depends on the constant k. For a probability p of about 99,7% (corresponding to 3σ) $k = 14.157\left(\text{and } \sqrt{k} = 3,763\right)$ for the 3d case as shown in Maybeck (1979), yielding semi-principal axes $\mathbf{e}_i = 3,763\sqrt{\lambda_i}\boldsymbol{\rho}_i$. Therefore the probability for the servicer not to be inside this ellipsoid is 0.3%.

4.2.2 Distance Calculation Ellipsoid to Client

In this section a new method will be introduced to verify that the client is in the error-ellipsoid of the servicer. Besides a pure yes/no indication information about the distance between the client and the servicer's error-ellipsoids surface is calculated. This safety distance is e.g. used in the iteration process.

4.2.3 Gradient Function

This chapter describes the calculation of the shortest distance between the ellipsoid's surface and the center of the client, which is based on the method shown by Eberly (2011). As the error-ellipsoid usually is skewed and displaced, the problem is transformed into a new frame, defined so that the semi-principal axis are aligned with the coordinate axis, with the associated extents e_i, $e_0 \ge e_1 \ge e_2 > 0$. The position of the client transformed into the new frame and thus the point to be examined is given by:

$$\mathbf{Y} = \left[y_0, y_1, y_2\right] = \left[\boldsymbol{\rho}_0, \boldsymbol{\rho}_1, \boldsymbol{\rho}_2\right]^{-1}(-\mathbf{r}) \quad (5)$$

where the eigenvectors $\boldsymbol{\rho}_i$ and the relative position vector $\mathbf{r}$ are sorted, so that they fit the semi-principal axes $\mathbf{e}_i$.

The surface of the error-ellipsoid is then given by $x_0^2 / e_0^2 + x_1^2 / e_1^2 + x_2^2 / e_2^2 = 1$ with $\mathbf{X} = \left[x_0, x_1, x_2\right]$ defining the ellipsoids surface. Based on the symmetry of the ellipsoid it is possible to restrict the problem into the first octant, $y_0 \ge 0, y_1 \ge 0, y_2 \ge 0$. The shortest vector from $\mathbf{Y}$ to $\mathbf{X}$ must be perpendicular to the ellipsoids surface. This is given for any gradient $\nabla G(x_0, x_1, x_2) = \left[2x_0^2 / e_0^2, 2x_1^2 / e_1^2, 2x_2^2 / e_2^2\right]$.

The distance from $\mathbf{X}$ to $\mathbf{Y}$ is thus obtained as:

$$\mathbf{Y} - \mathbf{X} = \tau \cdot \nabla G(x_0, x_1, x_2)/2 = \tau\left[x_0^2 / e_0^2, x_1^2 / e_1^2, x_2^2 / e_2^2\right] \quad (6)$$

for a scalar τ. The scalar τ indicates the direction (inwards or outwards) and qualitative the length of the vector from $\mathbf{Y}$ to $\mathbf{X}$. For $\tau > 0$ the point $\mathbf{Y}$ is outside the ellipsoid, otherwise it is inside (or on) the ellipsoid.

Equation (6) rewritten for x_i gives:

$$x_i = e_i^2 y_i / \left(\tau + e_i^2\right), i \in \left[1..3\right] \quad (7)$$

The solution of equation (7) has to be inside the first octant (ellipsoid symmetry) and thus $\tau > -e_0^2, \tau > -e_1^2, \tau > -e_2^2$. It is sufficient to examine $\tau > -e_2^2$, because $e_0 \ge e_1 \ge e_2$ are sorted.

To calculate τ with the result that $\mathbf{X}$ is closest to $\mathbf{Y}$, equation (7) is substituted into the ellipsoid equation:

$$F(\tau) = \left(\frac{e_0 y_0}{\tau + e_0^2}\right)^2 + \left(\frac{e_1 y_1}{\tau + e_1^2}\right)^2 + \left(\frac{e_2 y_2}{\tau + e_2^2}\right)^2 - 1 = 0 \quad (8)$$

The roots $F(\tau) = 0$ in the interval $I_\tau = (-e_2^2, \infty)$ are the candidates for the searched constant τ. There are one or more roots on the interval I_τ defined by the boundary conditions $\lim_{\tau \to -e_2^2} F(\tau) \to \infty,\ \lim_{\tau \to \infty} F(\tau) = -1$. On the interval I_τ the ellipse equation $F(\tau)$ is a continuous function and is at

least two times differentiable, with the first and second derivatives:

$$F'(\tau)=\frac{-2e_0^2y_0^2}{(\tau+e_0^2)^3}+\frac{-2e_1^2y_1^2}{(\tau+e_1^2)^3}+\frac{-2e_2^2y_2^2}{(\tau+e_2^2)^3}$$
$$F''(\tau)=\frac{6e_0^2y_0^2}{(\tau+e_0^2)^4}+\frac{6e_1^2y_1^2}{(\tau+e_1^2)^4}+\frac{6e_2^2y_2^2}{(\tau+e_2^2)^4}>0 \quad (9)$$

This implies that $F(\tau)$ is a convex function on I_τ thus the function has one unique root on the interval to be examined. This unique root yields the scalar τ. Thus the distance is calculated to:

$$d=\sqrt{(x_0-y_0)^2+(x_1-y_1)^2+(x_2-y_2)^2}=$$
$$\sqrt{y_0^2\left(\frac{e_0^2}{\tau+e_0^2}-1\right)^2+y_1^2\left(\frac{e_1^2}{\tau+e_1^2}-1\right)^2+y_2^2\left(\frac{e_2^2}{\tau+e_2^2}-1\right)^2} \quad (10)$$

Problems occur if y_2 is close to zero when $\lim_{t\to c}F(\tau)\to\infty$ is not true unless $c=-e_1^2$. Thus it is not possible to guarantee a root in the interval $I_\tau=(-e_2^2,\infty)$. This problem can be dealt with by a reduction to a 2D problem in such cases (not shown here).

4.2.4 Root Finding Algorithm

This chapter is about the root finding algorithm for $F(\tau)$ to get τ. A modified bisection method (MBM) is used followed by the standard Newton's method (NM). Just using the fast NM cannot guarantee convergence: Using an initial condition τ_0 with $F(\tau_0)<0$ has the possibility to cause an unstable process, where τ leaves the interval $I_\tau=(-e_2^2,\infty)$. Starting with a $\tau_0\in I_\tau$ with $F(\tau_0)>0$ guarantees convergence, because of the characteristics of a convex function on I_τ (see Equation 9) and the boundary conditions. Figure 1 shows a typical graph of $F(\tau)$.

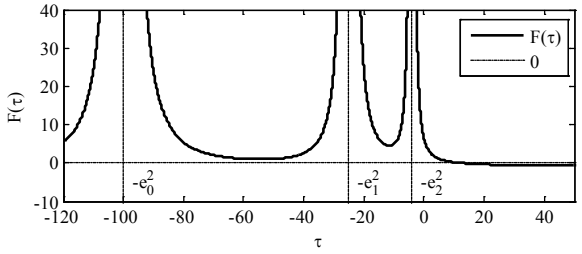

Figure 1: Typical graph of $F(\tau)$

The MBM is suited to determine such an initial condition because it is a stable root finding method in a bounded interval. $\tau_{\text{left}}=-e_2^2$ is used as left initial value any $\tau_{\text{right},1}>\tau_{\text{left}}$ is suitable. Here $\tau_{\text{right},1}=-e_2^2\sqrt{e_0^2y_0^2+e_1^2y_1^2+e_2^2y_2^2}$. The MBM calculates a new right value $\tau_{\text{right,i}}$ each step, until $F(\tau_{\text{right},i})>0$ using $\tau_{\text{right},i+1}=\left(\tau_{\text{left}}+\tau_{\text{right},i}\right)/2$. At each step the interval from τ_{left} to $\tau_{right,i}$ is divided into two intervals by computing the midpoint $\tau_{\text{right},i+1}$. In the standard method the subinterval which contains the root (identified by a conversion of the sign) is used. Here the MBM stops, as soon as the root is located in the right subinterval, where $F(\tau_{\text{right},i+1})>0$. This makes sure the calculated value $\tau_{\text{right},i+1}$ is left from the root and sufficient close to get guaranteed convergence with a NM with $\tau_{\text{Newton}}=\tau_{\text{right},i+1}$.

4.2.5 Collision Test

Finally the calculated distance between ellipsoid and client is evaluated and if the result is that the client is inside the ellipsoid, the following probability test is engaged.

4.3 Probability Test

The actual collision probility is computed by integrating a multivariate gaussian distribution defined by the servicer covariance and state. The integration volume is a box with dimensions given by the client and servicer satellite sizes and located at the origin.

This results in an approximation of the probability for the servicer hitting the client. Solving the integral is done using a triple integral approximation over the gaussian multivariate distribution function as described in Dan (2013).

This is a time consuming process but has to be computed only infrequently (when an ellipsoid collision is detected). If the collision probability is above some specific threshold (i.e. 1e-5) a warning is sent to the vehicle management. If a warning is triggered n consecutive times in a row the vehicle management commands a critical abort maneuver to move the servicer satellite to a predefined safe e/i separation.

5. PERFORMANCE

Performance of the collision prediction algorithm is demonstrated by testing a typical rendezvous approach for motion state safety in a complete and verified Matlab Simulink based satellite simulator developed by Astrium. A high order gravity model (30th order) and all major disturbance effects (i.e. airdrag which has the largest impact for an orbit altitude of 400km) are included.

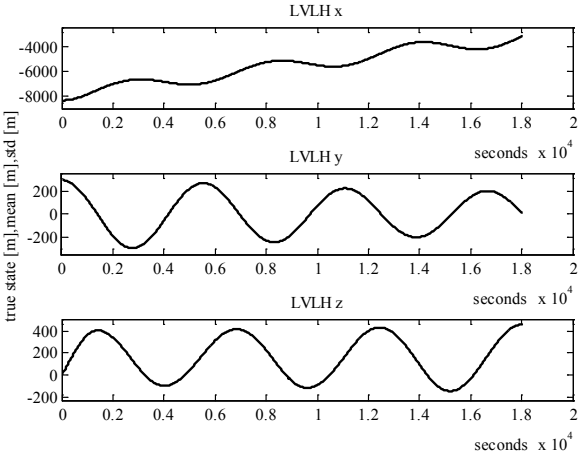

Figure 2: Example trajectory

After a short formation flying phase a drift motion is initiated and the servicer starts to approach the client. After 18000 seconds the servicer closed up to about 4 km behind the client as shown in Figure 2. The size of e/i separation is reduced during approach.

The initial navigation state and the initial covariance for each simulation step is taken from the navigation filter which is implemented as an absolute dynamics (ECI) based unscented kalman filter as shown in Posch et al. (2012).

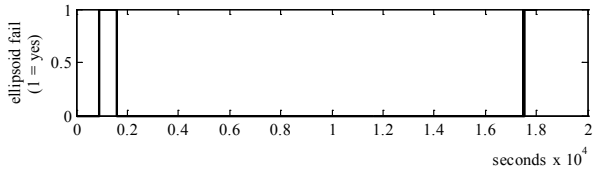

Figure 3: Safety Ellipsoid check fails

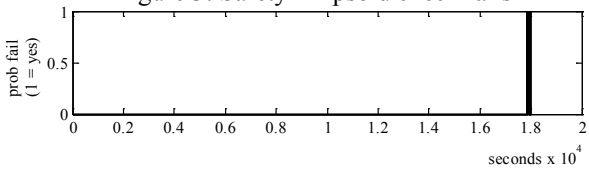

Figure 4: Safety probability check fails

Figure 3 and Figure 4 show the warning status of the two safety tests. As can be seen, the ellipsoid check fails during the maneuver to initiate the drift motion and then again when getting closer. The second test for probability shows acceptable collision probability for the first maneuver but throws a warning when getting closer. Figure 5 shows the minimum distances of ellipsoid to client, servicer to client and the maximum probability over time (which means the minimum / maximume for each tested time step). It has to be noted that the pure minimum servicer to client distance is no sufficient indicator for collision probability as it does not include the effect of navigation errors.

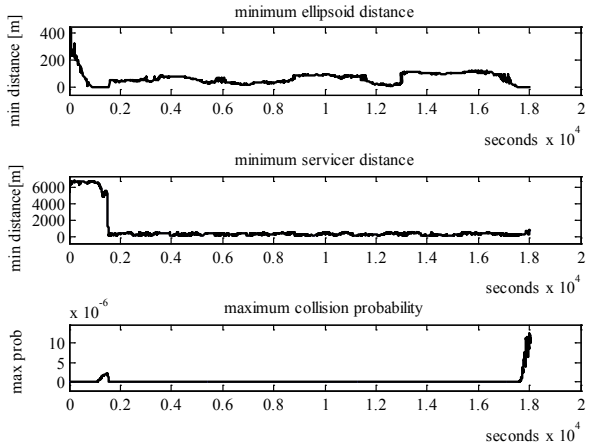

Figure 5: Safety test distances and probability

The safety test results for three time steps (t_{sim}) are shown in more detail now.

5.2 *No Collision*

This shows the prediction result for the no-warning case during drifting at time step 16200.

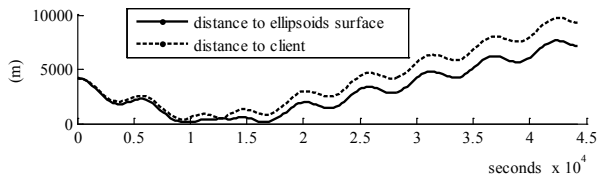

Figure 6: Distances (no collision case) t_{sim} = 16200

Figure 6 shows the evolution of the distance between ellipsoid and client and servicer and client over the prediction horizon of 8 orbits. It can be seen that the distance between ellipsoid and client is getting very small, but still above 0.

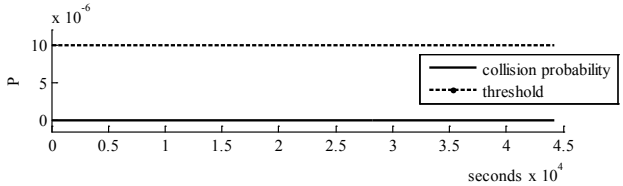

Figure 7: Collision prob. (no collision case) t_{sim} = 16200

The collision probability is therefore always very low as can be seen in Figure 7.

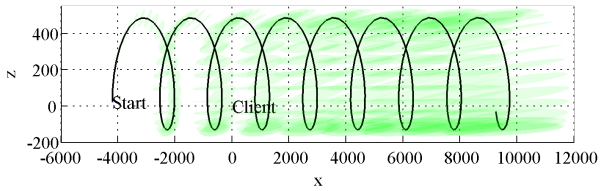

Figure 8: Trajectory and cov. (no collision case) t_{sim} = 16200

Figure 8 is a visualization of the covariance ellipsoid evolution (green) and the trajectory (black) for 8 orbits in 2d (LVLH x vs z). It can be seen that the navigation error becomes stretched primarily in along track direction. No hit is reported.

5.3 *Ellipsoid warning, probability ok*

This shows the prediction result for case when the ellipsoid test throws a warning while the probability is still ok, for example in the beginning at time step 1200 where the initial navigation error is quite big.

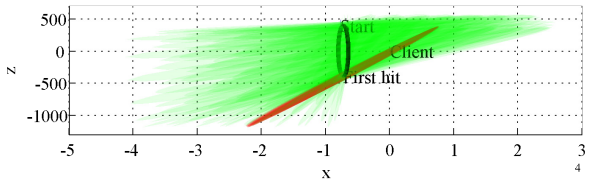

Figure 9: Trajectory and cov. (ellipsoid case) t_{sim} = 1200

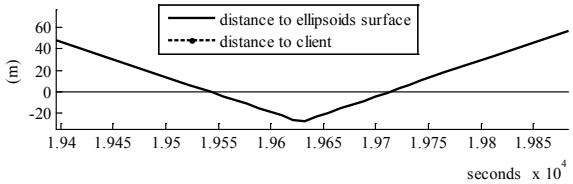

Figure 10: Distances (ellipsoid case) t_{sim} = 1200

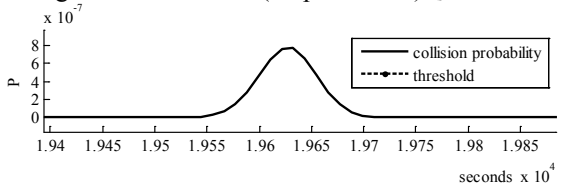

Figure 11: Collision probability (ellipsoid case) t_{sim} = 1200

As in the previous section, Figure 9 visualizes the evolution of the trajectory and the covariance over the prediction horizon. This time a collision warning for the ellipsoid is thrown (red).

Figure 10 displays only the relevant time period of the prediction which reports a hit after about 4 orbits. The maximum probability in this case is evaluated to about 8e-7, therefore no collision warning is reported (Figure 11).

5.4 Collision

This shows the prediction result for the case when both checks fail, e.g. in the end of the approach at t_{sim} = 18000.

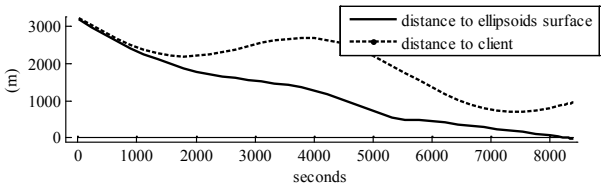

Figure 12: Distances (collision warn case) t_{sim} = 18000

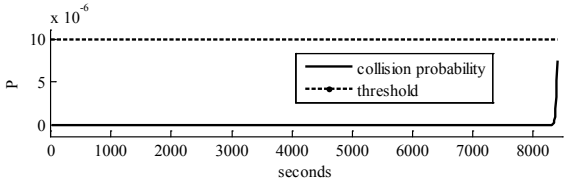

Figure 13: Collision probability (collision case) t_{sim} = 18000

Figure 12 shows the distances which indicate a ellipsoid hit after about 1.5 orbits. Figure 13 shows to probability which crosses the threshold and the prediction is immediately terminated (last evaluated step not shown).

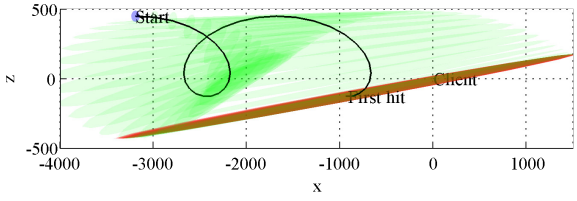

Figure 14: Trajectory and cov xz (collision case) t_{sim} = 18000

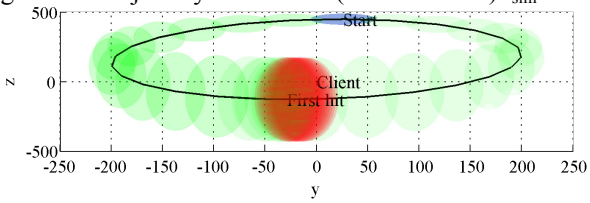

Figure 15: Trajectory and cov yz (collision case) t_{sim} = 18000

Figure 14 and Figure 15 show the prediction (in x-z and y-z planes) of the trajectory and the covariance ellipsoid which indicates a hit after 1.5 orbits.

5.5 Computational Effort

Several measures were undertaken to limit demands on the computation hardware: Using the direct solution with ROEs, employing an iterative approach for the trajectory testing, using a two step method (ellipsoid distance and probability integral) for the collision test and using fast methods to determine the ellipsoid distance (modified bisect and newton).

All that leads to a quite limited computational effort which can be further reduced by distributing the calculations for the collision test over a longer time span (e.g. evaluate every minute or before and after maneuvers or illumination changes). Evaluation for 8 orbits takes < 0.01s on one i7 core (~25k MIPS) which leads to ~2.5s execution time on a LEON3-FT (~100 MIPS, see Gaisler (2011)) or about 4% load when evaluated in one minute intervals. Thus it can be computed easily along with other GNC functionality and Onboard implementation is therefore feasible.

6. CONCLUSION

A new method for collision warning was presented that fits the requirements of current on-orbit rendezvous missions. It uses full 3d information and considers major disturbances like J2 and differential airdrag. Applying several methods to reduce computational effort gives feasibility of an onboard implementation.

Future work is on safety verification of orbit maneuver commands before they are executed and prohibiting them if they lead to unsafe conditions with collision risk.

ACKNOWLEDGEMENT

The work has been performed in close connection with Astrium GmbH and the author would thank Astrium GmbH for the cooperation and support doing this work.

REFERENCES

Akella, M., Alfriend, K. (2000). Probability of Collision Between Space Objects. Journal of Guidance, Control and Dynamics, Vol. 23, No. 5.

Barnhart, D. A. (2012). DARPA's Phoenix Project. DARPA On Orbit Satellite Servicing Workshop, GSFC, May 30, 2012.

D'Amico, S. (2010). Autonomous Formation Flying in Low Earth Orbit. *PhD thesis.* Technical University Delft.

D'Amico, S. (2005). Relative Orbital Elements as Integration Constants of Hill's Equations. DLR/GSOC, TN 05-08.

Dan, M. (2013). Numerical Triple Integral Approximation. *Website,* quantessence.files.wordpress.com/2012/01/tripleintegralapprox.pdf.

Eberly, D. (2011). Distance from a Point to an Ellipse, an Ellipsoid, or a Hyperellipsoid. Geometric Tools, LLC.

Gaisler, Aeroflex AB (2011). LEON3-FT Product Sheet. http://www.gaisler.com/doc/gr712rc-productsheet.pdf.

Harris, K., et al (2013). Application for RSO Automated Proximity Analysis and IMAging (ARAPAIMA): Development of a Nanosat-based Space Situational Awareness Mission. SmallSat 2013, Logan, Utah.

Hayman, Z. M. (2012). J2-Gravity Perturbed Motion of Artifical Satellite in Terms of Euler Parameters. The Open Astronomy Journal, Vol. 5.

Maybeck, P. (1979). Stochastic models, estimation, and control, New York: Academic Press Inc.

Montenbruck, O., Kirschner, M., D'Amico, S. (2004). E-/I-Vector Separation for Grace Proximity Operations. DLR/GSOC TN 04-08.

Posch, A., Schwientek, A. O., Sommer, J., Fichter, W. (2012). Comparison of filter techniques for relative state estimation of in-orbit servicing missions. IFAC Workshop on Embedded Guidance, Navigation and Control in Aerospace, Bangalore.

Reintsema, D., et al (2010). DEOS – The German Robotics Approach to Secure and De-Orbit Malfunctioned Satellites from Low Earth Orbits. i-SAIRAS 2010, Sapporo, Japan

Slater, G., Byram, S., Williams, T. (2006). Collision Avoidance for Satellites in Formation Flight. Journal of Guidance, Control and Dynamics, Vol. 29, No. 5.